Structural Analysis and Optimization of the Covalent Association between SpyCatcher and a Peptide Tag

Long Li[1], Jacob O. Fierer[2], Tom A. Rapoport[1] and Mark Howarth[2]

1 - *Howard Hughes Medical Institute and Department of Cell Biology,* Harvard Medical School, 240 Longwood Avenue, Boston, MA 02115, USA

2 - *Department of Biochemistry,* University of Oxford, South Parks Road, Oxford OX1 3QU, UK

Correspondence to Tom A. Rapoport and Mark Howarth: tom_rapoport@hms.harvard.edu; mark.howarth@bioch.ox.ac.uk
http://dx.doi.org/10.1016/j.jmb.2013.10.021
Edited by J. H. Naismith

Abstract

Peptide tagging is a key strategy for observing and isolating proteins. However, the interactions of proteins with peptides are nearly all rapidly reversible. Proteins tagged with the peptide SpyTag form an irreversible covalent bond to the SpyCatcher protein via a spontaneous isopeptide linkage, thereby offering a genetically encoded way to create peptide interactions that resist force and harsh conditions. Here, we determined the crystal structure of the reconstituted covalent complex of SpyTag and SpyCatcher at 2.1 Å resolution. The structure showed the expected reformation of the β-sandwich domain seen in the parental streptococcal adhesin, but flanking sequences at both N- and C-termini of SpyCatcher were disordered. In addition, only 10 out of 13 amino acids of the SpyTag peptide were observed to interact with SpyCatcher, pointing to specific contacts important for rapid split protein reconstitution. Based on these structural insights, we expressed a range of SpyCatcher variants and identified a minimized SpyCatcher, 32 residues shorter, that maintained rapid reaction with SpyTag. Together, these results give insight into split protein β-strand complementation and enhance a distinct approach to ultrastable molecular interaction.

Introduction

The tagging of proteins with peptides is one of the most widely used methods in protein detection, purification and immobilization [1–3]. In most cases, the peptide tag interacts reversibly, either with a protein, such as an antibody or a specific binding partner, or with a metal chelate. In contrast, the recently developed SpyTag/SpyCatcher tagging system involves the covalent attachment of a peptide tag to its cognate protein partner [4]. The system is based on the immunoglobulin-like collagen adhesion domain of *Streptococcus pyogenes* (CnaB2). CnaB2 contains an internal isopeptide bond [5] between amino acid residue Lys31 and residue Asp117 [6–8]. When CnaB2 is split into an N-terminal protein fragment containing Lys31 and a C-terminal peptide containing Asp117, the two fragments associate specifically and spontaneously form the isopeptide bond (Fig. 1a). A few modifications to the two binding partners made the reaction efficient both *in vitro* and *in vivo*. The modified

peptide and protein fragment were named SpyTag and SpyCatcher, respectively [4].

The SpyTag/SpyCatcher system offers several advantages over other tagging approaches. SpyTag (13 amino acids) forms a high-affinity initial non-covalent complex with its protein partner SpyCatcher (116 amino acids). The two partners then react rapidly, forming the isopeptide bond, with a half-time of 74 s for partners at 10 μM [4]. The reaction can take place in diverse conditions and is relatively insensitive to pH and temperature changes. Due to the covalent nature of the isopeptide bond, the SpyTag/SpyCatcher complex forms irreversibly and is stable to boiling in SDS or to forces of thousands of piconewtons [4]. The SpyTag can be placed at the N-terminus, at the C-terminus and at internal positions of a protein [4], in contrast to covalent peptide labeling via split inteins [9,10] or sortases [11]. Thus, the SpyTag/SpyCatcher system is potentially versatile and general. However, a better understanding of the interaction between the two partners is required to optimize the system.
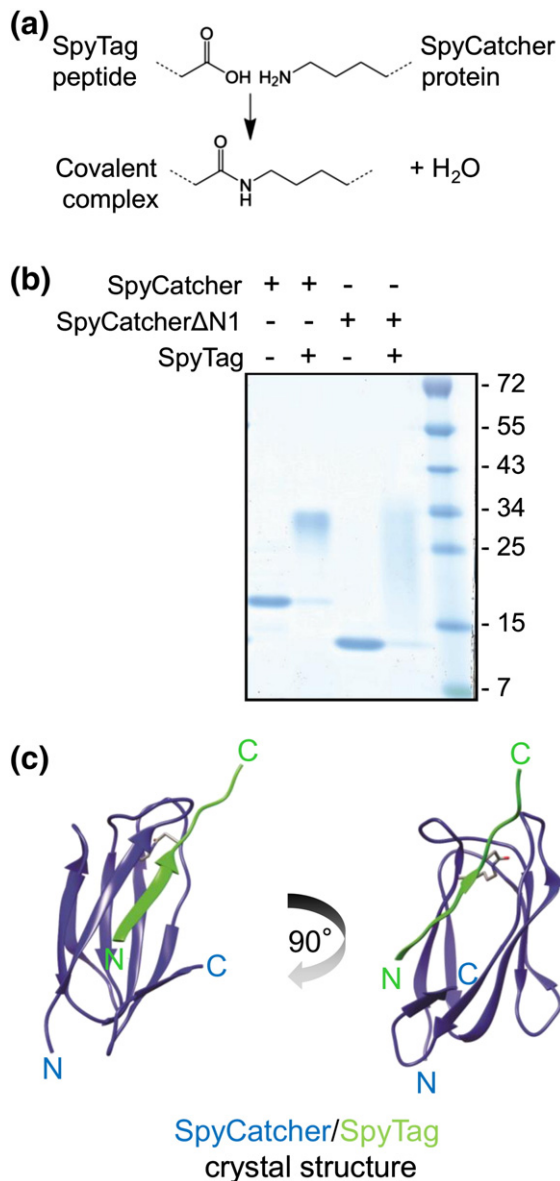
Fig. 1. Reconstitution of the SpyTag/SpyCatcher complex. (a) Chemistry of isopeptide bond formation between the reactive Asp of SpyTag and Lys of SpyCatcher. (b) Gel analysis of reaction between SpyTag and SpyCatcher or SpyCatcherΔN1. Tag and protein, both at 50 μM in phosphate-buffered saline, were incubated at room temperature for 1 h before boiling in SDS-loading buffer. The samples were analyzed by SDS-PAGE and Coomassie staining. (c) Ribbon diagram of the SpyTag/SpyCatcher crystal structure. SpyTag is colored green, and SpyCatcher is blue. The residues involved in the isopeptide are shown as sticks, with carbon atoms in gray. A second view of the structure is shown after 90° rotation.

Split proteins are an important and rapidly growing protein class, including split luciferase, fluorescent proteins, DNA polymerase and proteases. Split proteins give important insight into protein folding

and are powerful tools for logical computation or for reporting on diverse cellular events [12]. However, there are very few studies of how different split proteins reconstitute to form the original fold [13,14]. Here, we have analyzed the binding of SpyTag and SpyCatcher using X-ray crystallography and biochemical methods. The crystal structure of the SpyTag and SpyCatcher complex indicates that the N-terminal and C-terminal segments of SpyCatcher are dispensable for the interaction. Our biochemical and structural studies confirm that both termini could be deleted without a major effect on the structure or reaction rate. In addition, the crystal structure explains the effect of previously engineered point mutations on the reaction efficiency. Together, these results lead to an optimized and robust SpyTag/SpyCatcher system.

Results and discussion

Formation of a stable SpyTag/SpyCatcher complex

In preparation for crystallization trials, we used a synthetic peptide to test whether the isolated SpyTag can form a complex with SpyCatcher, as was previously shown for SpyTag-fusion proteins [4]. The SpyCatcher protein was purified as an N-terminal His-tagged protein by Ni-NTA chromatography after expression in *Escherichia coli* [4]. The His tag was removed by overnight digestion with the tobacco etch virus (TEV) protease. SpyCatcher protein was incubated with the SpyTag peptide at a 1:1 molar ratio at room temperature for 2 h, and the complex was further purified by anion-exchange and size-exclusion chromatography. The complex ran as a homogeneous species in both chromatography steps. However, in SDS gels, no distinct bands were seen; rather, the SpyTag/SpyCatcher complex smeared over a wide molecular weight range (Fig. 1b, lane 2), as was seen previously for the intact CnaB2 domain [7]. In contrast, SpyCatcher alone migrated as a distinct band (lane 1). These data suggest that the complex of SpyTag peptide and SpyCatcher is tightly folded, resisting unfolding by SDS. Similar results were seen for an N-terminally truncated version of SpyCatcher (SpyCatcherΔN1, see below) (Fig. 1b).

Crystal structure of the SpyTag/SpyCatcher complex

The SpyTag/SpyCatcher complex was very soluble and could be concentrated to more than 110 mg/ml (~7 mM) in a Tris–NaCl (pH 8) buffer. Initial trials with several commercially available screens gave no crystals. However, a cluster of thin-plate crystals appeared in a semi-dried drop with an elevated concentration of polyethylene glycol (PEG) 3350 after 1 month at 22 °C. These crystals were used for streak seeding and resulted in optimization of the crystallization conditions. The crystals grew into layers of thin plates. These crystals diffracted to a

Table 1. Data collection and refinement statistics

	SpyTag/SpyCatcher (PDB ID 4MLI)	SpyTag/SpyCatcherΔN1 (PDB ID 4MLS)
Data collection		
Wavelength (Å)	0.97920	0.97920
Resolution range (Å)	50 - 2.1 (2.14 - 2.1)	50 - 2.0 (2.03 - 2.0)
Space group	*P*1	*C*2
Unit cell dimensions		
a, b, c (Å)	31.62, 38.53, 44.49	71.13, 30.47, 39.88
α, β, γ (°)	83.70, 78.25, 89.72	90.00, 98.93, 90.00
Total reflections	15,926	16,321
Unique reflections	9604	5530
Multiplicity	1.7 (1.6)	3.0 (2.9)
Completeness (%)	80.5 (79.8)	94.4 (94.6)
Mean $I/\sigma(I)$	9.18 (5.02)	12.65 (5.23)
R_{merge}	0.072 (0.177)	0.117 (0.362)
Refinement		
R_{work}	0.198 (0.224)	0.210 (0.262)
R_{free}	0.225 (0.264)	0.237 (0.339)
RMSD (bond lengths, Å)	0.004	0.008
RMSD (bond angles, °)	0.68	1.11
Ramachandran favored (%)	97.6	98.9
Ramachandran outliers (%)	0	0

Statistics for the highest-resolution shell are shown in parentheses.
The SpyCatcher/SpyTag complex was concentrated to 110 mg/ml in 20 mM Tris and 50 mM NaCl (pH 8.0). Protein crystallization was performed in 24-well plates by hanging-drop vapor diffusion. We mixed 1 µl of the protein solution with 1 µl of the crystallization solution: 0.1 M sodium acetate (pH 4.5) and 30% PEG 3350. The crystallization drop was then streak seeded. The thin-plate crystals appeared in 1 day and grew to their full sizes in 3 days. The crystals were transferred to a drop of the cryo-solution containing the crystallization solution plus 5% glycerol before flash-freezing in liquid nitrogen. The SpyCatcherΔN1/SpyTag complex was crystallized similarly but without streak seeding. The complex was concentrated to 34 mg/ml, and the crystallization solution contained 0.1 M sodium acetate (pH 4.5), 200 mM NaCl, 30% PEG 3350 and 5% glycerol. The crystals were flash-frozen directly without using additional cryo-solution. The X-ray diffraction data were collected on beam ID-C of NE-CAT at the Advanced Photon Source in Chicago. The data were processed with HKL-2000 software (HKL Research Inc.) [15]. The structures were solved by molecular replacement with the program Phaser [16] and using the CnaB2 structure (PDB access number: 2X5P) as the search model. The refinement and final structure validation were performed with the program PHENIX [17]. The low multiplicity and data completion are due to the fact that the crystals consisted of several sub-crystals and that diffraction spots belonging to a single crystal had to be selected for data processing.

maximum of 1.7 Å, but it became clear that the diffraction spots were generated from multiple crystals. Because it was difficult to pick individual crystals, we carefully examined the diffraction pattern and selected for data processing the diffraction spots that belonged to a single crystal. The final structure was indexed to the *P*1 space group and was refined to a resolution of 2.1 Å (Table 1). Two molecules were located in the asymmetric unit, which were almost identical except for slight differences at the two termini of SpyCatcher. Coordinates and structure factors have been deposited in the Protein Data Bank (PDB ID 4MLI). One representative molecule (Chains A and B) is used for analysis in the following discussion.

SpyCatcher and SpyTag together form a compact β-sandwich structure (Fig. 1c). The first 12 of the 13 amino acids of SpyTag are visible in the density map. The electron density map clearly confirms the isopeptide bond between Lys31 of SpyCatcher and Asp7 of SpyTag (Figs. 1c and 2a) (numbering of SpyCatcher and variants based on PDB ID 2X5P). The first eight residues of SpyTag make interactions with the hydrophobic core of SpyCatcher (Fig. 2b):

the side chains of Ile3 and Met5 of SpyTag are inserted into a hydrophobic pocket formed by Phe29/Phe75/Phe92, Ile27/Ile90 and Met44 residues of SpyCatcher. SpyTag makes extensive parallel hydrogen bonds with β-strand 1 of SpyCatcher (residues 25–32), like the last β-strand of CnaB2. However, SpyTag contains five additional residues at the C-terminus. The hydroxyl group of Tyr9 participates in a hydrogen bond network involving Asp35 of SpyCatcher, a water molecule and possibly Lys37 (Fig. 2c). Lys10 of SpyTag electrostatically interacts with Glu85 of SpyCatcher. There is also a main-chain contact between Gly83 of SpyCatcher and Lys10 of SpyTag. The carboxylate group of Glu34 from SpyCatcher makes a hydrogen bond (distance ~ 2.7 Å) with the backbone NH of Tyr9 of SpyTag (Fig. 2c), which may explain why mutating Glu34 in SpyCatcher from Ile34 in CnaB2 [4] improved the efficiency of the reaction.

The interactions we see between Tyr9 and Lys10 of SpyTag and SpyCatcher rationalize the substantial improvement of the efficiency of SpyCatcher reaction comparing SpyTag (AHIVMVDAYKPTK) with a
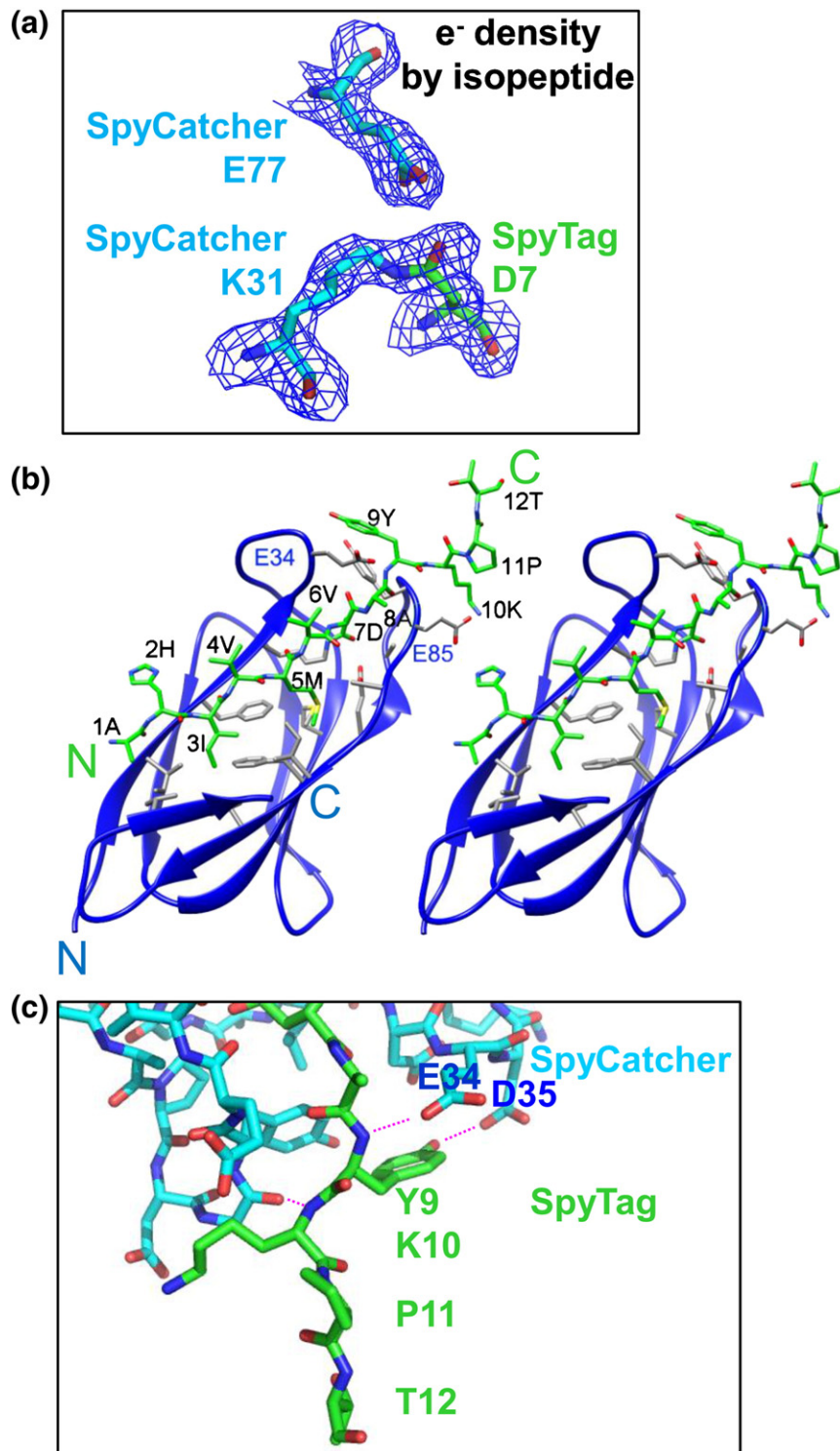
Fig. 2. Structural contacts between SpyTag and SpyCatcher. (a) Electron density confirmation of the isopeptide bond between SpyCatcher and SpyTag. Residues of the reactive triad are shown in stick format with the $2F_o - F_c$ map contoured at 1 σ overlaid. (b) Stereo diagram showing the interface between SpyCatcher and SpyTag. SpyCatcher is shown as blue ribbons, and the residues interacting with SpyTag are shown as sticks, with carbon atoms in gray. SpyTag is shown in green stick representation with its residues labeled. (c) Contacts between the tail of SpyTag (green) and SpyCatcherΔN1 (cyan). Putative hydrogen bonds are shown as magenta broken lines. Terminal residues of SpyTag and contacting residues of SpyCatcher are labeled.
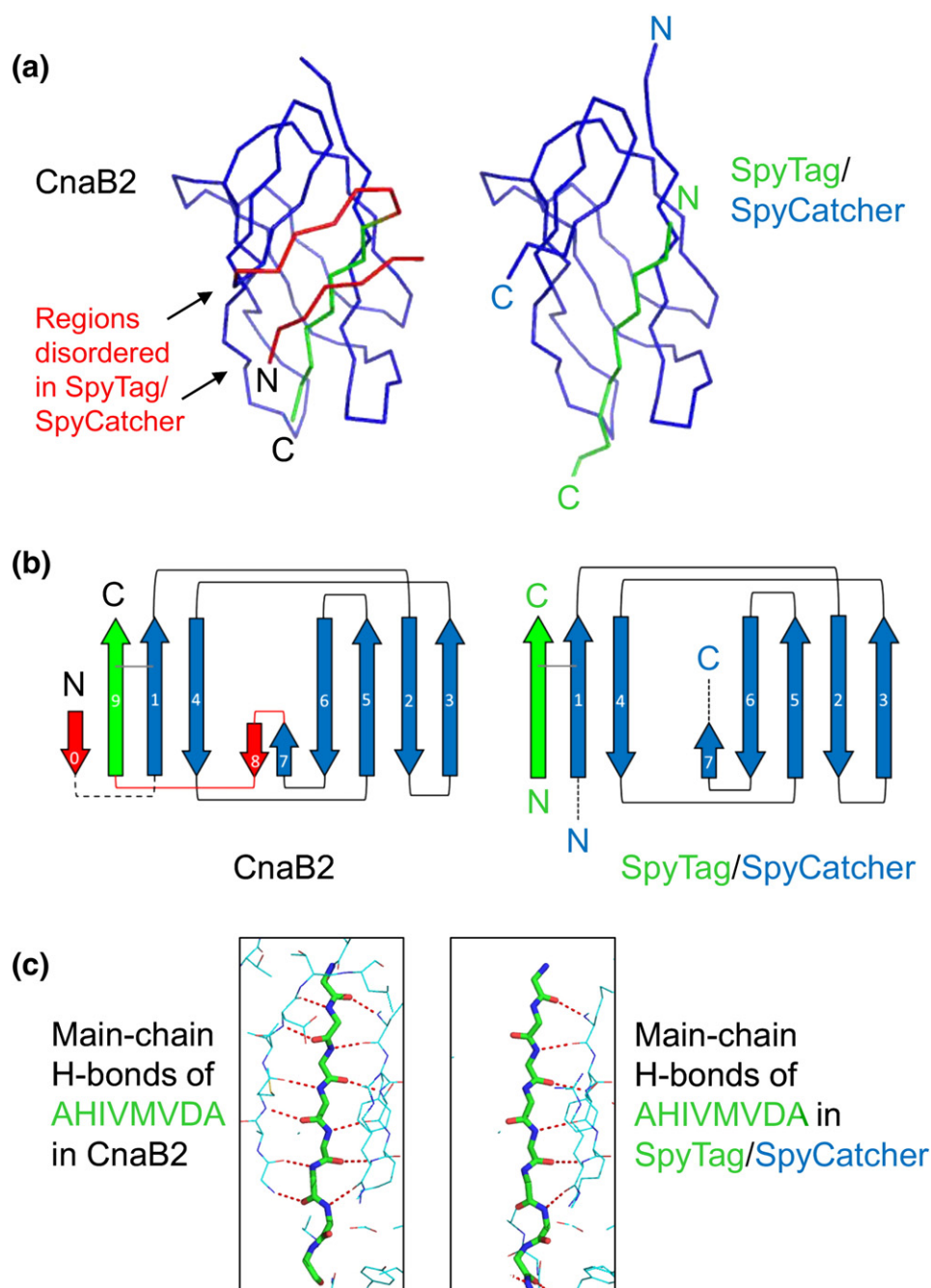
Fig. 3. Comparison between SpyTag/SpyCatcher and the intact CnaB2 domain. (a) Protein backbones are shown side-by-side in ribbon format, with SpyCatcher in blue and SpyTag in green. CnaB2 is shown in blue, except that regions that are resolved in the CnaB2 structure but disordered in the SpyTag/SpyCatcher structure are shown in red. The region corresponding to SpyTag in CnaB2 is highlighted in green. (b) Secondary structure diagram for CnaB2 and SpyTag/SpyCatcher. β-Strands are represented as arrows. Disordered peptides are shown as broken lines. The ordered segments in CnaB2 that are invisible in SpyTag/SpyCatcher are drawn in red. The isopeptide is colored gray. SpyTag and the corresponding region in CnaB2 are colored green. (c) Comparison of putative main-chain hydrogen bonding to the C-terminal strand of CnaB2 (left) or SpyTag (right), shown in green stick format, with hydrogen bonds as red broken lines. Residues from the rest of CnaB2 or SpyCatcher are shown in cyan line format.

peptide matching the original C-terminal sequence of CnaB2 (AHIVMVDA) [4]. However, our structures suggest that the three C-terminal amino acids of

SpyTag peptide (PTK) may not have a direct role in stabilizing the initial non-covalent complex between SpyTag and SpyCatcher: Pro11 and Thr12 are visible,
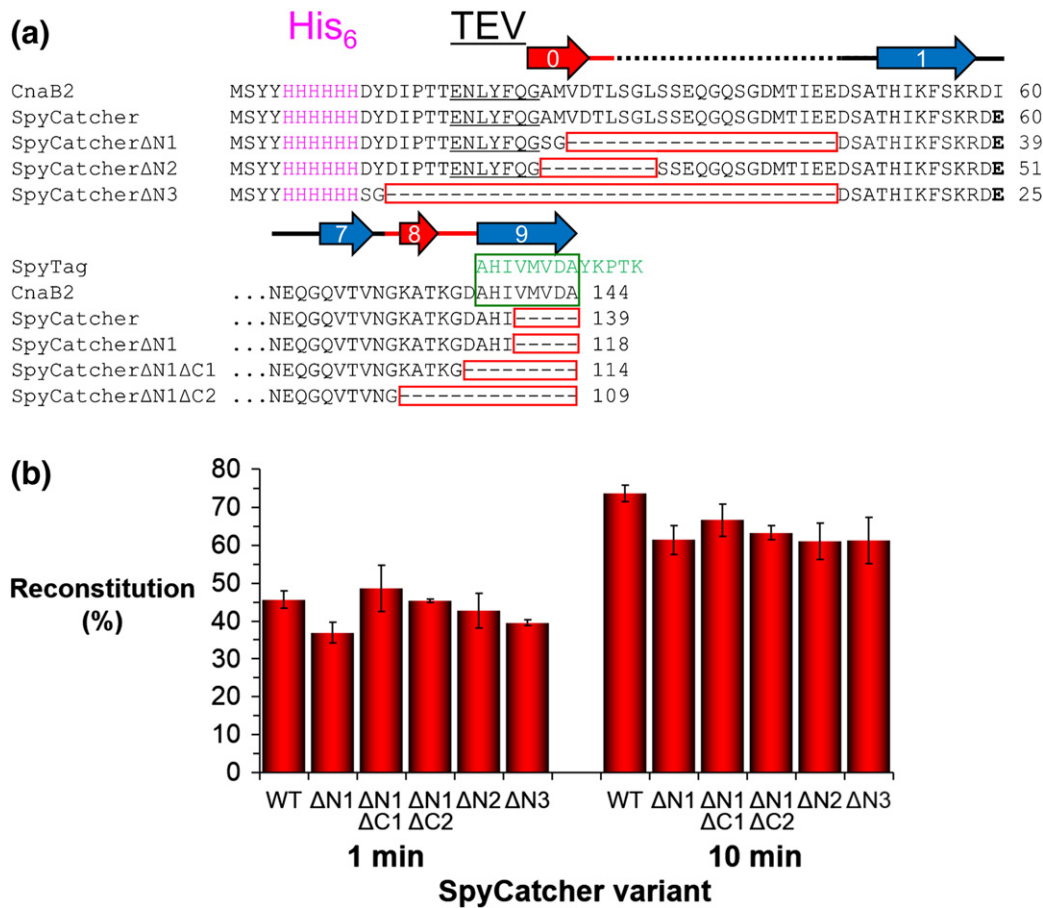
Fig. 4. Testing reaction rates of structure-based mutants of SpyCatcher. (a) Sequence alignment of the N-terminal and C-terminal regions of the SpyCatcher deletion mutants, compared to the parental CnaB2, SpyCatcher and SpyTag sequences. All the internal regions of the mutants are identical with SpyCatcher. Red and blue arrows correspond to β-strands marked in Fig. 3b. Red boxes indicate deleted regions in SpyCatcher mutants. SpyTag residues that are identical with the C-terminal region of CnaB2 are boxed in green. (b) Quantification of SpyCatcher variant reaction with SpyTag-MBP (mean of triplicate $\pm$ 1 SD from technical replicates). Each partner at 10 μM was incubated at 25 °C in 40 mM Na_2HPO_4 with 20 mM citric acid (pH 7.0) for 1 or 10 min, before adding SDS-loading buffer, heating at 95 °C for 7 min and analysis on SDS-PAGE with Coomassie staining before gel densitometry, as previously described [4]. Reconstitution was determined as 100× the band intensity of the covalent adduct, divided by the sum of intensities of the covalent adduct and SpyTag-MBP and the SpyCatcher variant.

but these two amino acids interact with residues of the neighboring SpyCatcher molecule in the crystal (Supplemental Fig. 1), while Lys13 is disordered.

Structural comparison of SpyCatcher/SpyTag and CnaB2

A comparison of the structures of the SpyTag/SpyCatcher complex and CnaB2 shows that the largest differences are at the terminal regions of the proteins (Fig. 3a and b). The structures are overlaid in Supplemental Fig. 2. In CnaB2 [6,7], the 6 N-terminal amino acids form a β-strand, whereas in the SpyTag/SpyCatcher complex, these residues are disordered. In both cases, the subsequent residues (amino acids 5–21) cannot be seen in the electron density map. Thus, in CnaB2 the β-strand of

the SpyTag is sandwiched between β-strands 0 and 1, whereas in the SpyTag/SpyCatcher complex the interaction with β-strand 0 is lost (Fig. 3b and c). Thus, N-terminal residues of SpyCatcher do not seem to contribute to the stability of the SpyTag/SpyCatcher complex. Complementation of a peptide into a groove surrounded on both sides by β-strands is sterically challenging. The SpyTag/SpyCatcher structure suggests that the binding site on SpyCatcher may be well exposed for docking of SpyTag, which may rationalize the much faster complementation of SpyTag/SpyCatcher compared to the related isopeptag/pilin-C spontaneous isopeptide bond-forming pair [18].

In the electron density map of the SpyTag/SpyCatcher complex, the backbone of SpyCatcher could be only traced to residue 103, leaving the

10 C-terminal residues of SpyCatcher disordered. In the CnaB2 structure, the first five residues of this segment form a short β-strand (strand 8) that is antiparallel with β-strand 7, and the last three residues are part of a β-strand that interacts with β-strands 0 and 1 (Fig. 3a and b). These last three residues are identical with the first three amino acids of SpyTag, which explains why peptide binding causes displacement of these residues from β-strand 1 and makes them disordered. This displacement is reminiscent of the donor-strand exchange seen in Gram-negative bacterial pilus assembly [19]. It is less clear why this difference would also cause the preceding β-strand of SpyCatcher to become disordered. In any case, our structure suggested that the C-terminal region of SpyCatcher might also be dispensable for interaction with SpyTag.

Temperature factors of CnaB2 and SpyCatcher/SpyTag structures cannot be directly compared because of the different resolutions (PDB ID 2X5P solved at 1.6 Å). However, normalization by the mean temperature factor of the main-chain atoms does give closely similar values over the major part of the CnaB2 and SpyCatcher structures, except for increased values for the C-terminal residues 97–103 of SpyCatcher (Supplemental Fig. 3). This comparison suggests that increased flexibility may extend into SpyCatcher's C-terminus even beyond the C-terminal residues that were not resolved at all.

The N-terminal and C-terminal segments of SpyCatcher are not required for efficient reaction with SpyTag

To test the prediction from our structures that the terminal segments of SpyCatcher are dispensable for the reaction with SpyTag, we first made N-terminal truncation mutants of SpyCatcher that lacked either 23 or 9 N-terminal residues (following the His tag and a TEV protease cleavage site, giving SpyCatcherΔN1 and SpyCatcherΔN2, respectively; Fig. 4a). We further generated a mutant from SpyCatcherΔN1 that lacked the TEV cleavage site (SpyCatcherΔN3). SpyCatcherΔN1-3 formed covalent complexes with SpyTag-MBP with similar efficiency to full-length SpyCatcher (~40% complex formation after 1 min and ~65% after 10 min; Fig. 4b).

To explore the role of the N-terminus structurally, we further analyzed SpyCatcherΔN1. SpyCatcherΔN1 efficiently formed a complex with SpyTag, which resisted unfolding by SDS (Fig. 1b). The SpyCatcherΔN1/SpyTag complex crystallized under similar conditions as SpyCatcher/SpyTag. As expected, the crystal structure of the SpyTag/SpyCatcherΔN1 complex at 2.0 Å resolution was almost identical with that of the non-truncated complex with an RMSD of 0.88 Å for all atoms (PDB ID 4MLS;

Table 1 and Supplemental Fig. 2). This result confirms that the N-terminus of SpyCatcher is dispensable for the interaction with SpyTag. There is always the possibility that a crystal structure captures one of many possible structural isoforms that exist in solution. Nevertheless, the close similarity between the structures of SpyTag with SpyCatcher and SpyCatcherΔN1 from different space groups adds to our confidence in the structural data.

Next, we generated two C-terminal deletions of SpyCatcherΔN1, removing either four or nine residues (SpyCatcherΔN1ΔC1 and SpyCatcherΔN1ΔC2, respectively; Fig. 4a). SpyCatcherΔN1ΔC1 and SpyCatcherΔN1ΔC2 were also able to react with comparable efficiency as the full-length SpyCatcher (Fig. 4b). Compared to wild-type SpyCatcher, the version with the largest deletion, SpyCatcherΔN1ΔC2, had only a 0.2% decrease in reconstitution at 1 min ($p = 0.88$, $n = 3$, not significant) and a 10.4% decrease in reconstitution at 10 min ($p < 0.005$, $n = 3$) (Fig. 4b) (two-tailed unpaired *t*-test performed using GraphPad). Thus, the biochemical data confirm that the 23 N-terminal and the 9 C-terminal amino acids can be removed from SpyCatcher without substantially affecting its reaction efficiency.

Taken together, our structural and biochemical data indicate that a minimal SpyTag/SpyCatcher system consists of residues 21–104 of the original SpyCatcher. The minimization of SpyCatcher from 116 amino acids to an 84-amino-acid core construct should enhance its applicability as a fusion tag for cellular expression, as well as taking its length firmly within the sequence range amenable to solid-phase peptide synthesis, thus facilitating chemical or isotopic modification [20].

One of the few split proteins investigated structurally is ribonuclease S, a functional enzyme generated by non-covalent interaction of a 20-amino-acid S peptide with a 104-amino-acid S protein. In contrast to SpyTag/SpyCatcher, S peptide forms an α-helix in the complex; also, apart from an eight-residue disordered stretch, ribonuclease S has a crystal structure identical within error with the intact parental protein [14]. The crystal structure of reassembled split Venus fluorescent protein did involve β-strand interactions, but both the two fragments were large and the difference to the intact protein was again small, with a main difference being two residues not forming a β-strand [13]. Therefore, our structures should contribute to the broad understanding of split protein complementation and the large number of residues that can have increased flexibility on reconstitution of certain complexes.

The optimized SpyTag/SpyCatcher system should be widely applicable for biochemical and cellular studies. By comparison with other tagging systems, SpyTag/SpyCatcher allows for a covalent interaction between the tag and the interacting recognition

molecule. While covalent bond formation often increases non-specific interactions, specificity is not compromised in the SpyTag/SpyCatcher system, as Lys and Asp have low intrinsic reactivity unless the residues are precisely aligned in the reactive triad. Because the interaction between SpyTag and SpyCatcher is irreversible, the linkage allows the purification of the tagged protein under stringent conditions. An interesting potential application of the SpyTag/SpyCatcher system is in the crystallization of membrane proteins. Our unpublished results show that the short SpyTag can be inserted into hydrophilic loops, and following folding and expression of the fusion protein, then SpyTag can react with recombinant SpyCatcher, to form a stable complex with increased hydrophilic surface for lattice-forming contacts. Such a system could have advantages over the insertion of large polypeptide domains into hydrophilic loops [21], which can affect the folding of membrane proteins.

Appendix A. Supplementary data

Supplementary data to this article can be found online at http://dx.doi.org/10.1016/j.jmb.2013.10.021.

References

[1] Jarvik JW, Telmer CA. Epitope tagging. Annu Rev Genet 1998;32:601–18.

[2] Lichty JJ, Malecki JL, Agnew HD, Michelson-Horowitz DJ, Tan S. Comparison of affinity tags for protein purification. Protein Expression Purif 2005;41:98–105.

[3] Terpe K. Overview of tag protein fusions: from molecular and biochemical fundamentals to commercial systems. Appl Microbiol Biotechnol 2003;60:523–33.

[4] Zakeri B, Fierer JO, Celik E, Chittock EC, Schwarz-Linek U, Moy VT, et al. Peptide tag forming a rapid covalent bond to a protein, through engineering a bacterial adhesin. Proc Natl Acad Sci U S A 2012;109:E690–7.

[5] Wikoff WR, Liljas L, Duda RL, Tsuruta H, Hendrix RW, Johnson JE. Topologically linked protein rings in the bacteriophage HK97 capsid. Science 2000;289:2129–33.

[6] Oke M, Carter LG, Johnson KA, Liu H, McMahon SA, Yan X, et al. The Scottish Structural Proteomics Facility: targets, methods and outputs. J Struct Funct Genomics 2010;11:167–80.

[7] Hagan RM, Bjornsson R, McMahon SA, Schomburg B, Braithwaite V, Buhl M, et al. NMR spectroscopic and theoretical analysis of a spontaneously formed Lys–Asp isopeptide bond. Angew Chem Int Ed Engl 2010;49:8421–5.

[8] Kang HJ, Baker EN. Intramolecular isopeptide bonds: protein crosslinks built for stress? Trends Biochem Sci 2011;36:229–37.

[9] Shi J, Muir TW. Development of a tandem protein trans-splicing system based on native and engineered split inteins. J Am Chem Soc 2005;127:6198–206.

[10] Volkmann G, Mootz HD. Recent progress in intein research: from mechanism to directed evolution and applications. Cell Mol Life Sci 2013;70:1185–206.

[11] Popp MW, Ploegh HL. Making and breaking peptide bonds: protein engineering using sortase. Angew Chem Int Ed Engl 2011;50:5024–32.

[12] Shekhawat SS, Ghosh I. Split-protein systems: beyond binary protein–protein interactions. Curr Opin Chem Biol 2011;15:789–97.

[13] Isogai M, Kawamoto Y, Inahata K, Fukada H, Sugimoto K, Tada T. Structure and characteristics of reassembled

fluorescent protein, a new insight into the reassembly mechanisms. Bioorg Med Chem Lett 2011;21:3021–4.

[14] Kim EE, Varadarajan R, Wyckoff HW, Richards FM. Refinement of the crystal structure of ribonuclease S. Comparison with and between the various ribonuclease A structures. Biochemistry 1992;31:12304–14.

[15] Otwinowski Z, Minor W. [20] Processing of X-ray diffraction data collected in oscillation mode. In: Carter CW, editor. Methods in Enzymology, New York: Academic Press; 1997. p. 307–26.

[16] McCoy AJ, Grosse-Kunstleve RW, Adams PD, Winn MD, Storoni LC, Read RJ. Phaser crystallographic software. J Appl Crystallogr 2007;40:658–74.

[17] Adams PD, Afonine PV, Bunkoczi G, Chen VB, Davis IW, Echols N, et al. PHENIX: a comprehensive Python-based system for macromolecular structure solution. Acta Crystallogr Sect D Biol Crystallogr 2010;66:213–21.

[18] Zakeri B, Howarth M. Spontaneous intermolecular amide bond formation between side chains for irreversible peptide targeting. J Am Chem Soc 2010;132:4526–7.

[19] Rose RJ, Welsh TS, Waksman G, Ashcroft AE, Radford SE, Paci E. Donor-strand exchange in chaperone-assisted pilus assembly revealed in atomic detail by molecular dynamics. J Mol Biol 2008;375:908–19.

[20] Kent SB. Total chemical synthesis of proteins. Chem Soc Rev 2009;38:338–51.

[21] Rosenbaum DM, Cherezov V, Hanson MA, Rasmussen SG, Thian FS, Kobilka TS, et al. GPCR engineering yields high-resolution structural insights into β2-adrenergic receptor function. Science 2007;318:1266–73.